Development Process of Thermal Convection Based on Water Surface Cooling with Aquatic Plants

Hamagami, Kunihiko
Department of Bioproduction and Environmental Sciences, Graduate School of Bioresource and Bioenvironmental Sciences, Kyushu University

Mori, Ken
Department of Bioproduction Environmental Sciences, Faculty of Agriculture, Kyushu University

Hirai, Yasumaru
Department of Bioproduction Environmental Sciences, Faculty of Agriculture, Kyushu University

https://doi.org/10.5109/10097

出版情報：九州大学大学院農学研究院紀要. 53 (1), pp.227-232, 2008-02-28. Faculty of Agriculture, Kyushu University
バージョン：
権利関係：

J. Fac. Agr., Kyushu Univ., **53** (1), 227–232 (2008)

Development Process of Thermal Convection Based on Water Surface Cooling with Aquatic Plants

Kunihiko HAMAGAMI[1], Ken MORI* and Yasumaru HIRAI

Laboratory of Bioproduction and Environment Information Sciences, Division of Bioproduction and Environment Information Sciences, Department of Bioproduction and Environmental Science, Factory of Agriculture, Kyusyu University, Fukuoka 812–8581, Japan
(*Received November 9, 2007 and accepted November 30, 2007*)

Hydraulic experiments were examined to investigate the characteristics of thermal convection based on inhomogeneous water surface cooling in a closed water body where aquatic plants grew thickly. We demonstrated the process of the generation and development of thermal convection from the results of water temperature measurement experiments. This explained the development process of convection was divided into three stages. Aquatic plants disturb the thermal transportation at the water surface, and the aspect ratio of the convection cell changes by the magnitude of the density difference near without the plants. Moreover, the development process of the thermal convection when the shield existed in the water surface was simulated by numerical experiment. As the result, it was clarified that the balance of the transportation equation of the turbulent energy.

INTRODUCTION

In some closed water bodies, hydraulic characteristics are different from those of river or irrigation canals because of insufficient inflow and outflow. When the water is undisturbed in a closed water body, the density stratification is formed in a vertical direction. In these bodies, the main fluid movement of the environmental substances is caused by based on thermal disturbance of the convective flow and mechanical disturbance of turbulent flow.

Recently, water quality problems have been studied with closed water bodies, including eutrophication (Lap *et al*., 2007). And water purification with aquatic plants has been proposed for several water bodies. The purification ability of aquatic plants is due to a filter effect with regard to suspended solids and an absorption effect with regard to nutrient salts. When aquatic plants grow on the water surface, the flow is affected by its luxuriant growth; therefore, it is important to elucidate the relationship between its luxuriant growth and fluid movement in a closed water body (Ozaki *et al*., 2004; Lap and Mori, 2007).

Many studies have reported on thermal convection at high Rayleigh numbers, and it has been found that the flow structure becomes irregular as the Rayleigh number increases. This phenomenon occurs in the vicinity of the bottom where a silicone rubber heater heats the water, or near the water surface, where it is cooled; this was determined by Spangenberg and Rowland (1970), Foster (1969), and Katsaros (1978) through various methods.

In this study, we focused on the generation and development processes of convective flow based on water surface cooling in a close water body with aquatic plants. And we clarified the generation and development processes of thermal convection and examined the influence by growing thickly of aquatic plants on the water surface by a hydraulic experiment. We then constructed a model for forecasting convective flow and examined the contribution of each term of the governing equation at each development stage.

METHODS AND RESULTS

Hydraulic experiment

Experiment equipment

The test tank was consisted of acrylic plates (length 60 cm, width 20 cm, depth 15 cm) (cf. Fig. 1). The bottom and sides of the test tank were covered with styrene foam boards 50 mm thick to prevent heat radiation. A thermocouple was used to measure water temperature. Thermocouples were set horizontally at 10 cm intervals from the inside 5 cm of the left side end of the tank and vertically at 1 cm intervals from 0.5 cm in depth which is defined as the surface in this experiment. The sampling frequency was 0.5 Hz. Air temperature was not controlled and measured by a mercury thermometer at a distance of 1 m from the test tank. We started water surface cooling when the temperatures difference of the air and the water became fixed difference. The influence of an aquatic plant was imitated by using the styrene foam. Plates of thickness 0.5 cm were set on the water surface at each end of the test tank. The experimental conditions are shown in Table 1. Rayleigh number was one of the experimental conditions. This number is defined as

$$R_a = \frac{\alpha g \Delta T H^3}{\kappa \nu} = \frac{\alpha g q H^4}{\rho C_p \kappa^2 \nu} \quad (1)$$

where α is the coefficient of thermal expansion (1/˚C);

[1] Laboratory of Bioproduction and Environmental Information Sciences, Division of Bioproduction and Environment Sciences, Department of Bioproduction Environmental Sciences, Graduate School of Bioresource and Bioenvironmental Sciences,Kyushu University

* Corresponding author (E–mail: moriken@bpes.Kyushu–u.ac.jp)

ΔT, the difference between air and water temperature (˚C); H, water depth (cm); κ, thermometric conductivity (cm^2/s); ν, the coefficient of kinematic viscosity (cm^2/s); q, heat flux ($cal/cm^2 \cdot s$); ρ, reference density (g/cm^3); C_p, specific heat (cal/g•˚C); and g, gravitational acceleration (cm/s^2). The parameters in Eq(1) were defined as $\alpha=2.5\times10^{-4}$, $g=980$, $\kappa=1.4\times10^{-4}$, and $\nu=0.01$.

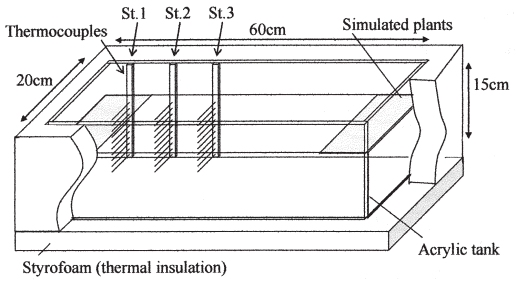

Fig. 1. Experimental equipment.

Table 1. Experimental conditions

EXP	coverage ratio	ΔT (°C)	Heat Flux q (cal/cm^2s)	Rayleigh number Ra
1–1	0%	15.1	9.33E–03	1.17E+11
1–2	0%	12.3	7.83E–03	9.79E+10
1–3	0%	10.1	5.79E–03	7.24E+10
2–1	10%	15.2	8.83E–03	3.88E+11
2–2	10%	12.3	6.62E–03	1.22E+11
2–3	10%	10.0	5.39E–03	7.97E+10
3–1	30%	15.0	9.83E–03	1.23E+11
3–2	30%	12.2	6.92E–03	8.65E+10
3–3	30%	10.1	5.12E–03	6.40E+10
4–1	50%	15.1	9.13E–03	3.90E+11
4–2	50%	12.3	7.57E–03	1.25E+11
4–3	50%	10.0	5.54E–03	8.00E+10

Experimental results and discussions

First of all, the characteristic of the water temperature variation of each depth in each measurement section is examined. Fig. 2 shows the variety of water temperatures at each depth in each measurement section in EXP3–1. In the figure, the temperatures were shifted down 0.3 ˚C successively in order to distinguish the variation at each measurement point. When coverage ratio is 30%, St.1, St.2 and St.3 are located in the cover, at the vicinity of the boundary and in the uncovered part, respectively, because aquatic plants were arranged at both ends.

A large variation is seen especially in the vicinity of the water surface, and the variation is growing also in the lower layer in the uncovered part (St.3). The water temperature begins to decrease after a while. From this, it is found that the temperature in the vicinity of the water surface change intensively by the thermal transportation at the water surface, and that the unstable state collapses and the cold water mass are then transported to the lower layer. In the covering part (St.1), the amplitude of water temperature is small compared with the uncovered part. But, the decrease rate of the water temperature in each measurement section is similar. It is found that the water cooled in the uncovered part flows to the covered part. That is, it is guessed that the horizontal convection is driven by a horizontal density difference.

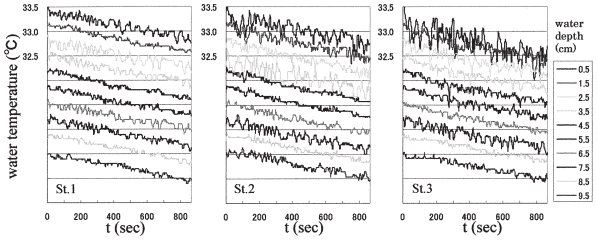

Fig. 2. The variation in water temperature in EXP3–1.

Fig. 3 shows the time variation in the calories of the water column per unit area in each measurement section. The calories in the column of the unit area of H depth were calculated by the formula,

$$Q=\int_0^H \rho c T dz \qquad (2)$$

where, T is water temperature (˚C); ρ, density of water (g/cm^3); c, specific heat of water. The approximate values $\rho=1.0$ and $c=1.0$ were used to calculate the calories. There is so no difference between each measurement sections in without coverage, and the value of St.3 is sometimes small in 10% coverage. In 30% and 50% coverage, though the calories decrease constantly in the covered part (St.1), they decrease rapidly in the initial stage in the uncovered part (St.3) and, afterwards, at almost the same rate of decrease as in the covered part. That is, cold water mass forms near the water surface in the uncovered part, causing temperatures below the surface to fall. Afterwards, horizontal convection occurs as a result of the temperature difference with the covered part, and the colder temperature is transported horizontally.

Fig. 4 shows the turbulent intensity of the water temperature variation at 0.5 cm in depth in each measurement section. In this figure, $\hat{T}$ is the turbulent inten-

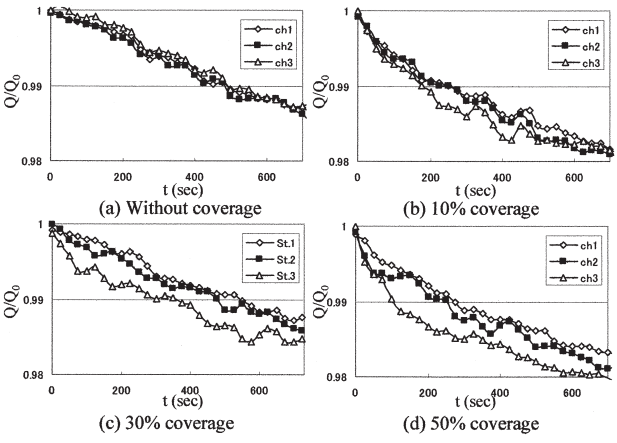

Fig. 3. The time variation in the calories of the water column per unit area.

sity (˚C); T_0, the initial water temperature (˚C). This calculation revealed a tendency in each section for turbulent intensity to increase when the heat flux of the water surface increases in each coverage rate. There are not so many differences in without coverage and 10% coverage. The turbulent intensity of the covered part (St.1) is smaller than that of the uncovered part (St.3), and that of the boundary part (St.2) takes roughly a middle value in 30% and 50% coverage. In without coverage and 10% coverage, St.1 and St.2 are not covered. But St.1 is covered and St.2 is near the boundary part in 30% and 50% coverage. Thus, it is found that the coat obstructs the transportation of heat, and that the generation of turbulent by unstable density becomes small. We then used the wavelet conversion to examine the characteristics of water temperature variation in detail.

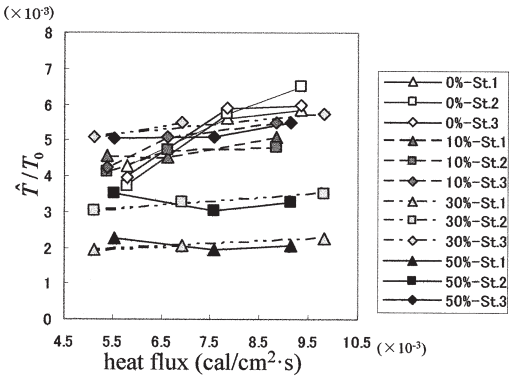

Fig. 4. The turbulent intensity of water temperature variation.

Fig. 5 shows the wavelet conversion chart of the water temperature variation at 0.5 cm in depth in each measurement section in EXP3–1. We conducted a discrete wavelet transform using the Daubechies mother wavelet as the analyzing wavelet. The wavelet coefficient is expressed in the formula.

$$\omega_k^{(j)} = 2^{-j/2}\int_{-\infty}^{\infty} f(t)\overline{\psi(2^{-j}t-k)}dt \qquad (3)$$

Where ω is the wavelet coefficient; f, data function; ψ, mother wavelet function; t, time; k, the position (or time); j, level. The color display expresses the magnitude of the wavelet coefficient at each coordinate. The vertical axis corresponds to frequency and the horizontal to elapsed time. We used the turbulent element of the water temperature variation for the analysis.

As the results, the dominant frequency band of the water temperature variation changes as time passes in the development stage in each measurement section. In the initial stage, a high–frequency band is dominant. That is, it is shown that the generation of detailed cold water mass frequently generated. The dominant frequency band became small as for the development stage, and it is found that the developing plume generated regularly. Moreover, the dominant frequency band in the uncovered part (St.3) becomes smaller that that in the covered part (St.1) in the initial stage. That is, a steady plume is formed because the heat transportation is large in the uncovering part. Also, the boundary part (St.2)

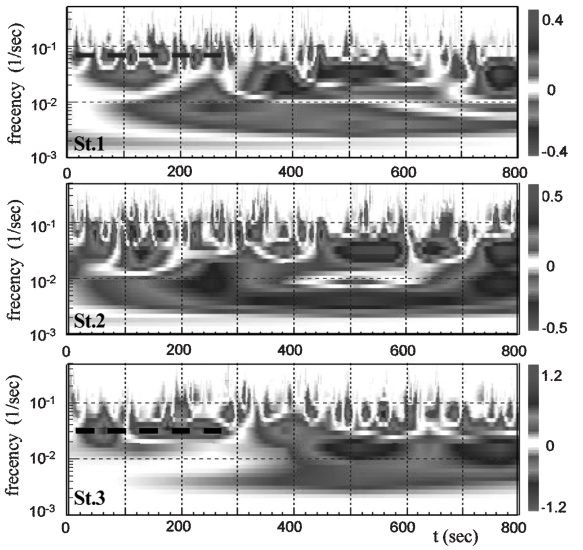

Fig. 5. Wavelet conversion chart of water temperature variation in EXP3–1.

shows the variation characteristics in which both of the surrounding dominant frequency bands appear; it is thought that coexistence of both frequency bands is influenced by the water exchange between the covered part and the uncovered part.

Numerical experiment

Governing equations of thermal convection

Fig. 6 shows the calculation area. We assumed a simple rectangular water body with a 10 cm depth H and a 60 cm length L. The x axis was set horizontally, and the z axis vertically. The governing equations of a Boussinesq fluid motion in a two–dimensional rotating frame under rigid–lid approximation are the equation of continuity (4) and the equation of motion ((5), (6)),

$$\frac{\partial(\rho u)}{\partial x} + \frac{\partial(\rho w)}{\partial z} = 0 \qquad (4)$$

$$\frac{\partial}{\partial t}(\rho u) + \frac{\partial}{\partial x}(\rho u \cdot u) + \frac{\partial}{\partial z}(\rho w \cdot u) = -\frac{\partial p}{\partial x} + \frac{\partial}{\partial x}\left(\mu_{eff}\frac{\partial u}{\partial x}\right) + \frac{\partial}{\partial z}\left(\mu_{eff}\frac{\partial u}{\partial z}\right) + S_U \qquad (5)$$

$$\frac{\partial}{\partial t}(\rho w) + \frac{\partial}{\partial x}(\rho u \cdot w) + \frac{\partial}{\partial z}(\rho w \cdot w) = -\frac{\partial p}{\partial z} + \frac{\partial}{\partial x}\left(\mu_{eff}\frac{\partial w}{\partial x}\right) + \frac{\partial}{\partial z}\left(\mu_{eff}\frac{\partial w}{\partial z}\right) - \rho g + S_V \qquad (6)$$

where u and w are the velocity in x and z directions; p, pressure deflection from hydrostatic pressure at the constant density ρ_0=1.0 g/cm^3 (ρ is assumed to be only a function of temperature); α, coefficient of thermal expansion, μ_{eff} is the effect viscosity, and to which a turbulent viscosity coefficient μ_t was added coefficient of viscosity μ. Moreover, the generation paragraphs S_U and S_V are given by the following formulae.

$$S_U = \frac{\partial}{\partial x}\left(\mu_{eff}\frac{\partial u}{\partial x}\right) + \frac{\partial}{\partial z}\left(\mu_{eff}\frac{\partial w}{\partial x}\right) \qquad (7)$$

$$S_V = \frac{\partial}{\partial z}\left(\mu_{eff}\frac{\partial w}{\partial z}\right) + \frac{\partial}{\partial x}\left(\mu_{eff}\frac{\partial u}{\partial z}\right) \tag{8}$$

The turbulent flow model, the k–ε model, is adopted, and the transportation equations of the turbulent energy k and the energy dissipation rate ε are as follows.

$$\frac{\partial}{\partial t}(\rho k) + \frac{\partial}{\partial x}(\rho u \cdot k) + \frac{\partial}{\partial y}(\rho w \cdot k) - \frac{\partial}{\partial x}\left(\frac{\mu_{eff}}{\sigma_k}\frac{\partial k}{\partial x}\right) - \frac{\partial}{\partial z}\left(\frac{\mu_{eff}}{\sigma_k}\frac{\partial k}{\partial z}\right) = G - \rho\varepsilon \tag{9}$$

$$\frac{\partial}{\partial t}(\rho \varepsilon) + \frac{\partial}{\partial x}(\rho u \cdot \varepsilon) + \frac{\partial}{\partial z}(\rho w \cdot \varepsilon) - \frac{\partial}{\partial x}\left(\frac{\mu_{eff}}{\sigma_\varepsilon}\frac{\partial \varepsilon}{\partial x}\right) - \frac{\partial}{\partial z}\left(\frac{\mu_{eff}}{\sigma_\varepsilon}\frac{\partial \varepsilon}{\partial z}\right) = C_1\frac{\varepsilon}{k}G - C_2\rho\frac{\varepsilon^2}{k} \tag{10}$$

$$G = \mu_t\left\{2\left[\left(\frac{\partial u}{\partial x}\right)^2 + \left(\frac{\partial w}{\partial z}\right)^2\right] + \left(\frac{\partial u}{\partial z} + \frac{\partial w}{\partial x}\right)^2\right\} \tag{11}$$

Where C_1=1.44, C_2=1.92, σ_k=1.0, σ_ε=1.3, C_μ=0.09. The wall function was applied as a boundary condition in the bottom and the sidewall. Moreover, for the turbulent energy k_S and the energy dissipation rate ε_S in the water surface,

$$k_S = \frac{{u_{*S}}^2}{{C_\mu}^{1/2}}, \quad \varepsilon_S = \frac{{C_\mu}^{3/4}{k_S}^{3/2}}{\kappa \Delta y_S} \tag{12}$$

where u_{*S} is the water surface friction velocity; κ, a Kalman constant; and Δy_S, depth from the water surface of the definition point. The temperature diffusion equations is,

$$\frac{\partial}{\partial t}(\rho cT) + \frac{\partial}{\partial x}(\rho cuT) + \frac{\partial}{\partial z}(\rho cwT) = \frac{\partial}{\partial x}\left(c\mu_T\frac{\partial T}{\partial x}\right) + \frac{\partial}{\partial z}\left(c\mu_T\frac{\partial T}{\partial z}\right) - \frac{dQ_z}{dz} \tag{13}$$

where T is a water temperature; c, isopiestic specific heat; μ_T, the coefficient of eddy diffusion; Q_z, heat flux in the water surface.

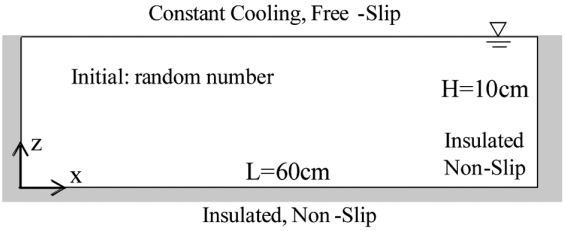

Fig. 6. Model area with boundary and initial conditions.

Development process of convection cells

Fig. 7 shows the temperature distribution and the stream line chart at each development stage in the case of no coverage. At the beginning of water surface cooling, a thermal boundary layer was formed near the water

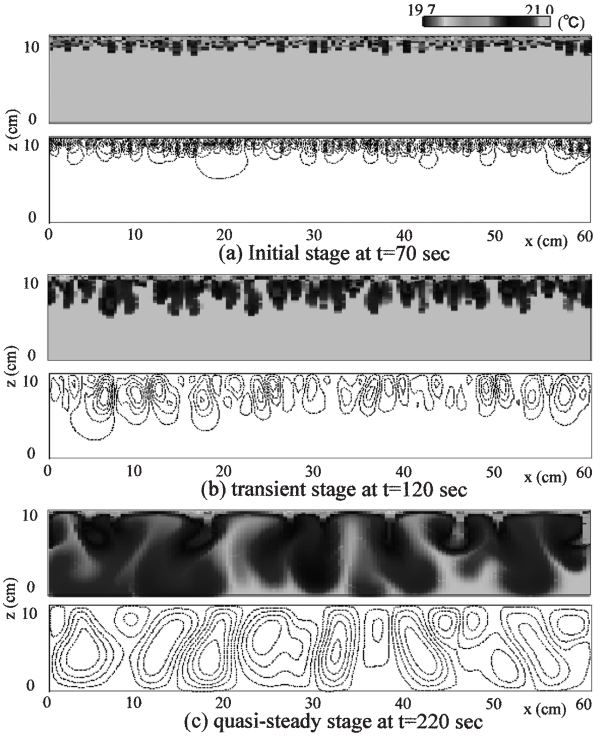

Fig. 7. The temperature distribution and the stream function in without coverage.

surface, and it is found a lot of small convection cells have been generated from the stream line chart. When the cold water mass falls in the thermal and a clear convection cell is formed, this can be called the initial stage of mixture layer development. These cells increase the scale vertically and horizontally. This stage, where the convection cell absorbs or annexes each other, and the horizontal scale is increased, can be called a transient stage. And then, the convection cell continues in a comparatively steady state. This can be called the quasi–steady stage.

Fig. 8 shows the temperature distribution and the stream line chart in the case of 30% coverage. At the initial stage, the convection cell develops in the uncovered part, but no significant convection is generated in the covering part. Also, at the transient stage, a large convection cell is centered near the boundary. At the quasi–steady stage, the aspect ratio of the convection cell is larger, and it is shown that a horizontal flow caused by the density difference as a result of covering the water surface. From these results taken together, it can be said that this model can excellently reproduce the effect of water surface coverage on thermal convection.

The effect of the coverage was examined in detail by considering the balance of the transportation equation of the turbulent energy. Fig. 9 shows the balance of the transportation equation of the turbulent energy at each development stage in without coverage. At the initial stage, the contribution of unsteady term and generation term is large. It is thought that the potential energy added by the heat transportation from the water surface is transported vertically by the subsidence of the cold

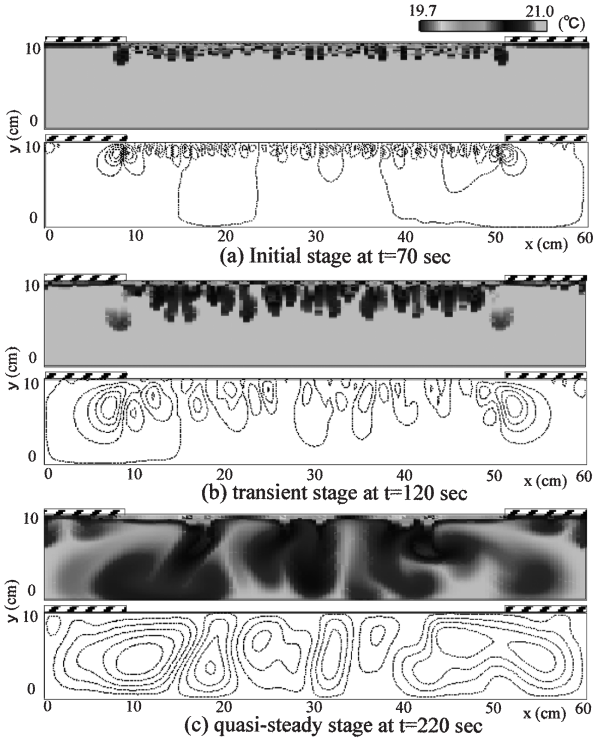

Fig. 8. The temperature distribution and the stream function in 30% coverage.

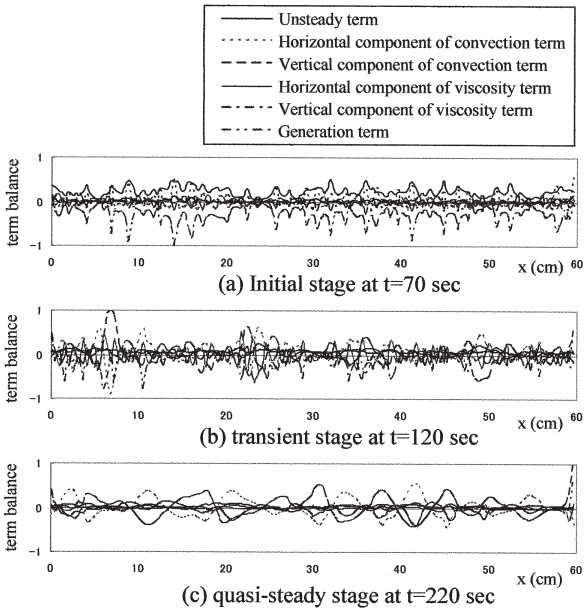

Fig. 9. The term balance of the transportation equation of the turbulent energy in without coverage.

water mass at this stage. At the transient and quasi–steady stage, the contribution of horizontal and vertical component of convection term is growing. The convection cell is generated intermitting at this stage, and unsteady term has become small.

Fig. 10 shows the balance of the transportation equation of the turbulent energy at each development stage in 30% coverage. At the initial stage, any term hardly has the value in the coating part, and it is found that the turbulent energy does not transported. At the

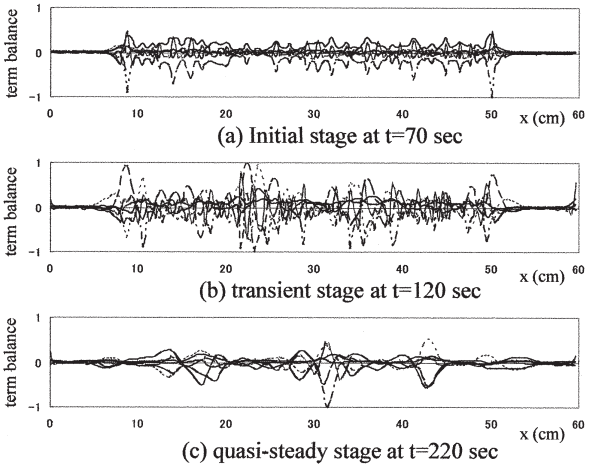

Fig. 10. The term balance of the transportation equation of the turbulent energy in 30% coverage.

transient stage, horizontal component of convection term contributes in the coating part. After that, other terms of vertical component of convection term etc. also contribute to the transportation of turbulent at the quasi–steady stage. That is, as for the development of the convection cell in the covering part, a horizontal flow by the density difference is dominant.

CONCLUSION

We discussed the development process of thermal convection from the hydraulic experiment and the numerical experiment. The following results about the effect of covering on the water surface were obtained.

(1) The generation and development process of thermal convection is classified into an initial stage, where a lot of cold water mass are generated near the water surface; a transient stage, where convection cell develop its vertical and horizontal scale; and a quasi–steady stage, where the convection cell keep to a steady state.

(2) The development process of the heat convection is greatly influenced when there is a covering in the water surface. Because the heat transportation of the water surface is small in the covering part, a density difference was formed horizontally. Then aspect ratio of the developing convection cell is large.

ACKNOWLEDGEMENTS

The authors wish to thank Laboratory of Drainage and Water Environment, Division of Regional Environmental Science, Department of Bioproduction Environment Science, Faculty of Agriculture, Kyushu University for the convenience in the conducting the experiment.

REFERENCES

Asaeda, T., N. Tamai, Y. Takahashi 1982 On the thermal con-

vection of an equilibrium state for large water depth and large Rayleigh number. *Proceedings of the Japan Society of Civil Engineers*., **323**: 121–131

Asaeda, T., N. Tamai, 1983 On characteristics of plumes observed in the thermal convection with the large Rayleigh number. *Proceedings of the Japan Society of Civil Engineers*., **336**: 65–73

Foster, T. D. 1969 Onset of manifest convection in a layer of fluid with a time–dependent surface temperature. *Phys. Fluids*., **12**: 2482–2487

Katsaros, K. B. 1978 Turbulent free convection in fresh and salt water : some characteristics received by visualization. *J. Phys. Ocean*., **3**: 613–626

Lap, B. Q., K. Mori and E. Inoue, 2007 A one–dimensional model for water quality simulation in medium– and small–sized rivers. *Paddy Water Environ*., **5(1)**: 5–13

Lap, B. Q. and K. Mori, 2007 A two–dimensional numerical model of wind–induced flow and water quality in closed water bodies. *Paddy Water Environ*., **5(1)**: 29–40

Ozaki, A., K. Mori, E. Inoue and T. Haraguchi, 2004 Impact of Aquatic Plants on Entrainment Phenomena Based on Wind–Induced Flow in a Closed Density Stratified Water Area. *Paddy Water Environ*., **2**: 125–134

Spangenberg, W. G. and W. R. Rowland 1970 Convective circulation in water induced by evaporating cooling. *Phys. Fluids*., **4**: 793–800